Preprints.org

Article

Not peer-reviewed version

# Hydrodynamic and Mass-Transfer Modeling of Uranium Recovery in a Packed Ion-Exchange Column with a Conical Flow Distributor

Aidarkhan Kaltayev *, Zhomart Ualiev , Asylkhan Bibossinov

Posted Date: 27 March 2026

doi: 10.20944/preprints202603.2235.v1

Keywords: uranium sorption; packed column; porous media; hydrodynamics; convective–dispersion transport; flow distributor; numerical modeling

Preprints.org is a free multidisciplinary platform providing preprint service that is dedicated to making early versions of research outputs permanently available and citable. Preprints posted at Preprints.org appear in Web of Science, Crossref, Google Scholar, Scilit, Europe PMC.

Copyright: This open access article is published under a Creative Commons CC BY 4.0 license, which permit the free download, distribution, and reuse, provided that the author and preprint are cited in any reuse.

Preprints.org (www.preprints.org) | NOT PEER-REVIEWED | Posted: 27 March 2026 doi:10.20944/preprints202603.2235.v1

Disclaimer/Publisher's Note: The statements, opinions, and data contained in all publications are solely those of the individual author(s) and contributor(s) and not of MDPI and/or the editor(s). MDPI and/or the editor(s) disclaim responsibility for any injury to people or property resulting from any ideas, methods, instructions, or products referred to in the content.

*Article*

# Hydrodynamic and Mass-Transfer Modeling of Uranium Recovery in a Packed Ion-Exchange Column with a Conical Flow Distributor

**Aidarkhan Kaltayev [1,2,*], Zhomart Ualiev [1] and Asylkhan Bibossinov [3]**

[1] Joldasbekov Institute of Mechanics and Engineering, Shevchenko st. 28, Almaty 050010, Kazakhstan

[2] Kazakh National Technical University named after K.I. Satpayev, st. Satpayev 22, Almaty 050000, Kazakhstan

[3] JSC "NCGNTE", st. Bogenbay batyr, 221, Almaty 050026, Kazakhstan

* Correspondence: aidarkhan.kaltayev@gmail.com; Tel.: +7 777 721 20 20

**Abstract**

Efficient recovery of uranium from productive leaching solutions requires a clear understanding of hydrodynamic and mass-transfer processes in ion-exchange sorption columns. In this study, a coupled hydrodynamic and mass-transfer model is developed to investigate uranium sorption in a packed ion-exchange column equipped with a conical flow distributor. Fluid flow in the porous resin bed is described by the Forchheimer filtration law combined with the mass conservation equation, while transport of dissolved uranium species is modeled using a convective–dispersion equation coupled with a sorption kinetics equation based on the linear driving force approximation. Numerical simulations are performed using the fictitious domain method to represent the complex geometry of the column. The pressure field is determined using the Ritz variational method, and the transport equation is solved with the Crank–Nicolson scheme. The results show that uranium distribution between liquid and solid phases forms a ring-shaped region inside the column, indicating uneven utilization of the sorbent bed. It is also found that the conical flow distributor does not fully eliminate radial flow non-uniformity. Doubling the solution flow rate increases the width of the mass-transfer zone by about 1.5 times due to enhanced longitudinal dispersion. The proposed approach can be used to analyze and optimize industrial sorption columns for uranium recovery.

**Keywords:** uranium sorption; packed column; porous media; hydrodynamics; convective–dispersion transport; flow distributor; numerical modeling

## 1. Introduction

Many deep or shallow deposits of rare and valuable metals are currently extracted using the in-situ leaching (ISL) method because of its cost-effectiveness and relatively low environmental impact [1–6]. In this process, uranium-bearing minerals are dissolved underground and transported to the surface in productive solutions, commonly called pregnant leach solutions. During processing, sorption–precipitation methods are widely employed to concentrate valuable components directly at mining sites using ion-exchange resins [7–9].

Existing studies on uranium sorption mainly focus on modeling transport processes and sorption kinetics in fixed-bed columns, considering advection, hydrodynamic dispersion, and physicochemical interactions between uranium species and sorbents [10–13].

This study examines the ion-exchange extraction dynamics of dissolved uranium species from pregnant leach solutions in a complex-geometry packed sorption column, using mathematical and numerical modeling. Such columns are commonly employed in the uranium industry for extracting uranium from productive solutions [11,12].

© 2026 by the author(s). Distributed under a Creative Commons CC BY license.

Preprints.org (www.preprints.org) | NOT PEER-REVIEWED | Posted: 27 March 2026 doi:10.20944/preprints202603.2235.v1



First, the design of the sorption column is described. Then, based on experimental data obtained in a packed column, the kinetic characteristics of the sorbent are determined. The corresponding kinetic coefficients are estimated by fitting calculated and experimental concentration profiles of uranium in the liquid phase at different cross-sections of the column. These parameters are subsequently used in the mathematical model describing the transport of dissolved uranium species and their sorption in the porous sorbent bed.

At the final stage, the efficiency of the sorption column operation is analyzed using the fictitious domain method and numerical simulations in order to investigate the influence of the conical flow distributor geometry.

The present study considers the first cycle of the sorption column operation, in which the sorbent initially does not contain uranium species. Modeling of periodic operation of the column would require additional information on the residual uranium distribution in the sorbent after unloading the saturated layer.

## 2. Materials and Methods

### *2.1. Description of the Sorption Column*

The design and operating scheme of the packed sorption column (SK, hereafter referred to as the column or sorber), widely used in uranium mining enterprises of Kazatomprom, is shown in Figure 1. The column represents a cylindrical vessel of height $H$ and radius $R$ with a truncated conical bottom. In the lower part of the column, upstream of the feed pipe with diameter $d$, a conical flow distributor is installed. Its purpose is to reduce the non-uniformity of the hydrodynamic flow and the corresponding concentration distribution of uranium species over the cross-section of the column.

The column is densely packed with a fixed bed of granular ion-exchange resin (Purolite). The sorbent consists of porous spherical particles with diameter $\delta$ and a highly developed internal surface. The particle diameter is several orders of magnitude smaller than the diameter of the feed pipe and the column diameter $D=2R$. Therefore, the sorbent bed can be treated as a porous medium with porosity $\phi$.

The pregnant leach solution containing dissolved uranium species (primarily uranyl ions $UO_2^{2+}$ or their complexes) enters the column from below through the feed pipe at a constant volumetric flow rate $Q_0$. During the ion-exchange process, mobile hydrogen ions of the resin are replaced by uranium ions from the solution, resulting in the ion-exchange reaction

$$2R - H + UO_2^{2+} \rightleftharpoons 2R_2U_2 + 2H^+, \quad (1)$$

because the binding energy of uranium ions with the resin is higher than that of hydrogen ions

$$E(resin - U) > E(resin - H).$$

Here $R$ denotes the active functional group of the resin, $R - H$ represents the resin in the hydrogen form, $R_2U_2$ is the uranyl complex $UO_2^{2+}$ fixed on the resin, and $H^+$ is the hydrogen ion released into the solution.

Due to the developed internal structure of the resin granules and the small size of the capillaries inside them, the ion-exchange process between the solution and the sorbent is mainly controlled by intraparticle diffusion.

© 2026 by the author(s). Distributed under a Creative Commons CC BY license.

Preprints.org (www.preprints.org) | NOT PEER-REVIEWED | Posted: 27 March 2026 doi:10.20944/preprints202603.2235.v1



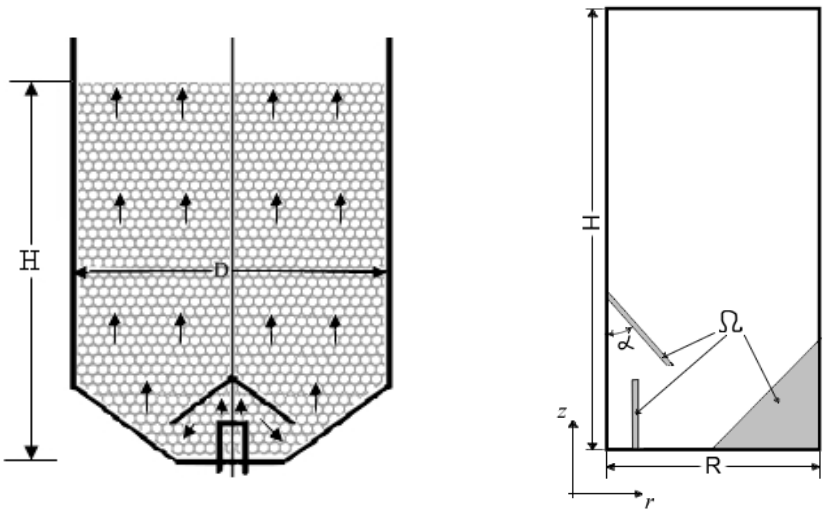


**Figure 1.** Scheme of the SK sorption packed column.

Before entering the sorbent bed, the flow passes through the conical distributor with opening angle $\alpha$, defined as the angle between the column axis and the generatrix of the distributor.

During column operation, solution samples are periodically collected from the top outlet of the column and analyzed for uranium concentration. The sorption process continues until the average uranium concentration in the outlet solution reaches a specified limit value. At this stage, the lower part of the sorbent bed that has become saturated with uranium is removed, fresh sorbent is added from the top of the column, and the sorption cycle is repeated.

*2.2. Mathematical Model and Numerical Solution*

The pregnant leach solution containing dissolved uranium species consists predominantly of water and, under the considered conditions, can be approximated as an incompressible Newtonian fluid with density and viscosity close to those of water.

Because the characteristic size of the resin particles is much smaller than the column diameter, the sorbent bed is densely packed and immobile, and the flow velocities are relatively low, the flow of the solution through the sorbent layer is considered as filtration flow in a porous medium.

Due to the narrow particle size distribution and nearly spherical shape of the ion-exchange resin granules, and assuming uniform packing of the column, the sorbent bed can be treated in a macroscopic approximation as a homogeneous and isotropic porous medium characterized by effective filtration properties.

Because the sorption column and the inlet pipe are axisymmetric, the fluid flow and the sorption process are also assumed to be axisymmetric. Consequently, the three-dimensional transport of the pregnant solution and the mass-transfer process in the column can be reduced in cylindrical coordinates ($r$, $\theta$, $z$) to an axisymmetric two-dimensional problem (Figure 1b).

Near the inlet pipe and the conical flow distributor, the Reynolds number may significantly exceed unity, whereas in the main part of the column, the flow retains a filtration character. Therefore, the motion of the fluid in the porous sorbent bed is described using the relations of filtration theory — the Forchheimer equation and the mass conservation equation for fluid in the pore space [14–17]:

$$\alpha\vec{u}(r,z,t) = \alpha\phi\vec{v}(r,z,t) = -\nabla P(r,z,t), \quad (2)$$

$$\nabla\cdot\vec{u} = \nabla\cdot(\phi\vec{v}) = 0, \quad (3)$$

where $\vec{u}(r,z,t)$ is the Darcy velocity, $\phi$ is the bed porosity, $\vec{v}(r,z,t)$ is the average fluid velocity in the pores, $\alpha = \alpha_1 + \alpha_2|\vec{u}|$, $P=p/\rho + \vec{g}\cdot\vec{x}$, $p$ is the fluid pressure, $\rho$ is the fluid density, $\vec{g}$ is the

© 2026 by the author(s). Distributed under a Creative Commons CC BY license.

Preprints.org (www.preprints.org) | NOT PEER-REVIEWED | Posted: 27 March 2026 doi:10.20944/preprints202603.2235.v1



gravitational acceleration, $\vec{x}$ is the position vector, $\mu$ is the dynamic viscosity of the solution, δ is the diameter of spherical sorbent particles,

$\alpha_1 = 633\mu(1-\phi)/\rho\delta^2$ , $\alpha_2 = 3(1-\phi)\phi/2\theta\delta$.

For typical porosity values $\phi \leq 0.4$, it is assumed that the empirical coefficients satisfy the relations given by Goldshtik (1984):

$\theta = 0.508 - 0.56(1-\phi)$.

The transport of dissolved uranium species in the pregnant leach solution and the ion-exchange process between the liquid solution and the sorbent are assumed to be isothermal and are described by the following partial differential equation [12,13,16–19]:

$$\partial C/\partial t + \nabla \cdot (\vec{v}\, C) = \nabla \cdot (D\nabla C) - (\varphi^{-1} - 1)\ \partial \bar{C}/\partial t\ , (4)$$

where $D$ is the hydrodynamic dispersion tensor.

Because the porous medium is assumed to be homogeneous and isotropic, the dispersion tensor is symmetric and has three non-zero components [14,15]:

$$D_{rr} = \alpha_L \frac{v_r^2}{|\vec{v}|} + \alpha_T \frac{v_z^2}{|\vec{v}|} + D_m,$$

$$D_{zz} = \alpha_T \frac{v_r^2}{|\vec{v}|} + \alpha_L \frac{v_z^2}{|\vec{v}|} + D_m,$$

$$D_{rz} = D_{zr} = (\alpha_T - \alpha_L)\frac{v_r v_z}{|\vec{v}|},$$

where $\alpha_L = \mathrm{C}_1|\vec{v}|$ is the longitudinal dispersion coefficient proportional to the sorbent particle diameter, $\alpha_T = \mathrm{C}_2|\vec{v}|$ is the radial dispersion coefficient, $\alpha_L/\alpha_T \approx 5, D_m$ is the molecular diffusion coefficient in the liquid phase.

The fluid velocity field appearing in the transport equation is determined as follows.
From the Forchheimer relation, the magnitude of the velocity is expressed as a function of the pressure gradient magnitude. The velocity vector can therefore be written as

$$\vec{u} = -\nabla P/(\alpha_1 + \alpha_2 f(|\nabla P|)\ . (2')$$

Substituting this expression into the mass conservation equation (3) in cylindrical coordinates yields a nonlinear elliptic equation for the pressure field:

$$\frac{\partial}{\partial r}\left(rA\frac{\partial P}{\partial r}\right) + \frac{\partial}{\partial z}\left(rA\frac{\partial P}{\partial z}\right) = 0\ (5)$$

where

$$A(r,z,t) = 1/(\alpha_1 + \alpha_2 f(|\nabla P|).$$

After solving Equation (5), the velocity field in the sorption column is obtained from Equation (2′).

The ion-exchange process between the solution and the sorbent according to scheme (1) is assumed to be controlled by intraparticle diffusion and is described by the **pseudo-first-order kinetic equation** [9,18,20,21]:

$$\partial \bar{C}/\partial t = \beta(C - \bar{C}/K_d)\ , \qquad (6)$$

where

$\bar{C}$ is the concentration of uranium species adsorbed by the sorbent,

$C$ is the concentration of dissolved uranium species in the solution,

$\beta$ is the kinetic coefficient of sorption characterizing the rate of intraparticle mass transfer,

$K_d$ is the equilibrium distribution coefficient.

For the fluid velocity and pressure at the solid walls of the column the **no-flux boundary condition** is imposed:

© 2026 by the author(s). Distributed under a Creative Commons CC BY license.

Preprints.org (www.preprints.org) | NOT PEER-REVIEWED | Posted: 27 March 2026 doi:10.20944/preprints202603.2235.v1



$$\alpha\vec{u}\cdot\vec{n}|_S = -\partial P/\partial n|_S = 0, \quad (7)$$

where $\vec{n}$ is the unit normal vector to the column wall.

At the column inlet the cross-sectional area of the feed pipe, the volumetric flow rate, and the inlet concentration of dissolved uranium species are specified:

$$\vec{u}\cdot\vec{n}|_{in} = \partial P/\partial z|_{in} = V_0 = Q_0/S_{in}\,, C|_{in} = C_{in}. \quad (8)$$

At the column outlet the pressure is assumed equal to the ambient pressure, and soft boundary conditions are imposed on the concentration distribution:

$$P|_{out} = P_{out}, \partial C/\partial z|_{out} = 0 \ . (9)$$

At the initial time the column is filled with liquid and fresh sorbent that does not contain uranium species:

$$C(\vec{x}, t=0) = 0, \bar{C}(\vec{x}, t=0) = 0 \ . (10)$$

The kinetic parameters $\beta$ and $K_d$ n Equation (6) were determined by fitting the numerical results to experimental sorption data obtained for ***Purolite*** **ion-exchange resin.**

The sorption kinetic curves obtained from experimental measurements were used to determine the kinetic characteristics of the sorbent, including the equilibrium time, sorbent capacity at equilibrium, the equilibrium distribution coefficient, and the kinetic sorption coefficient (Figure 2). Considering the sorption process in the experiment as a mass-transfer process occurring in an ideal reactor, the following parameter values were obtained: $\beta \approx 120\ h^{-1}$ и $K_d$=286.

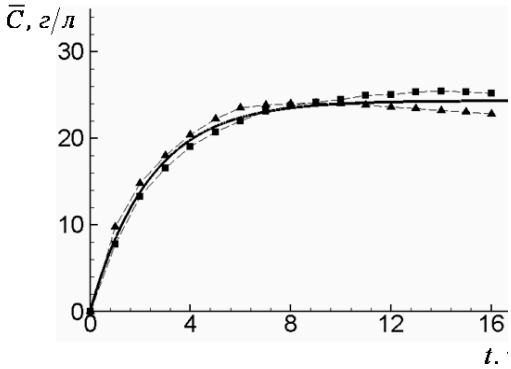


**Figure 2.** Experimental and calculated sorption kinetics of uranium on *Purolite* resin.

Among numerical methods for solving problems of mathematical physics, the finite-difference method is one of the most universal approaches. From a computational point of view, this method is most efficiently implemented on regular grids in domains with simple geometries, such as rectangles or their combinations. However, in numerical studies of mass-transfer processes accompanied by physicochemical reactions in domains of complex shape, the finite-element method or the finite-volume method is more commonly applied [22–24].

Alongside these approaches, the fictitious domain method (FDM) has been widely used in recent years to solve problems in irregular computational domains [25–28]. In the fictitious domain method, the original problem defined in the irregular physical domain Ω s extended to a regular computational domain *R*, which is formed as the union of the physical domain Ω and the fictitious domain $\Omega_f$ (Figure 3):

$$R=\Omega \cup \Omega_f \ .$$

The theoretical convergence of the method is associated with the fulfillment of a uniform **inf–sup condition**, which leads to a compatibility condition between the boundary grid and the uniform computational grid [25]. Another important aspect is that the stability condition of the resulting numerical scheme is similar to the stability conditions of conventional finite-difference schemes.

© 2026 by the author(s). Distributed under a Creative Commons CC BY license.

Preprints.org (www.preprints.org) | NOT PEER-REVIEWED | Posted: 27 March 2026 doi:10.20944/preprints202603.2235.v1



Within the fictitious domain method, the boundary conditions are extended into the fictitious region as follows. For terms containing first-order derivatives (convective terms), the extension is performed along the flow direction, i.e., according to the lower-order derivative. For second-order terms (dispersion–diffusion terms), the extension is performed according to the higher-order derivative, which ensures a correct approximation of derivatives at the boundary [25].

For the solution of the elliptic pressure equation (4), a coefficient $A_\varepsilon$ is introduced in the fictitious domain method, defined as

$$A_\varepsilon = H(\vec{x})rA + \big(1 - H(\vec{x})\big)\varepsilon, (11)$$

where

$$H(\vec{x}) = \begin{cases} 1, \vec{x} \in \Omega \\ 0, \vec{x} \in \Omega_f \end{cases}$$

is the **Heaviside function**, and $\varepsilon$ is a small parameter., $\varepsilon \ll rA$. As a result, the solution of the pressure equation

in the irregular physical domain Ω with Neumann boundary conditions is reduced to solving the following equation in the regular computational domain *R*:

$$\partial(A_\varepsilon\, \partial P/\partial r)/\partial r + \partial(A_\varepsilon\, \partial P/\partial z)/\partial z = 0. (12)$$

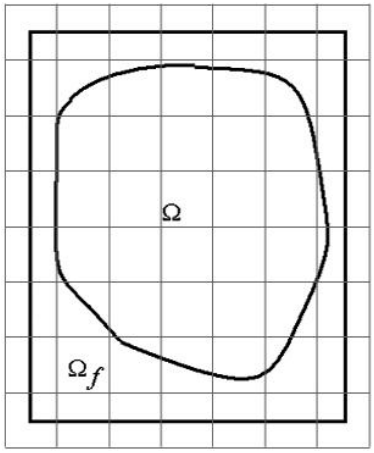


**Figure 3.** Schematic representation of the physical and computational domains in the fictitious domain method. The computational domain is defined as R=Ω ∪ $\Omega_f$, .

The pressure field and its derivatives are extended into the fictitious domain in such a way that a consistent approximation of the second-order derivatives at the interface between the physical and fictitious domains is ensured. In particular, for the Neumann problem for pressure on the physical boundary ∂Ω, the following compatibility conditions are imposed:

$$[P(\vec{x}, t)]_{\partial\Omega} = 0, \left[\sum_{ij=1}^{2} n_i A_\varepsilon\, \partial P/\partial x_j\right]_{\partial\Omega} = 0, (13)$$

where $\vec{n}$ is the outward unit normal vector to the boundary $\partial\Omega$, and the notation $[\cdot]_{\partial\Omega}$ denotes the jump of a function across the interface between the physical and fictitious domains.

The transport equation for dissolved uranium species in the regular domain *R* takes the form

$$\partial C/\partial t + \nabla \cdot (\vec{v}\, C) = \nabla \cdot (D_\varepsilon \nabla C) - (\phi^{-1} - 1)H(\vec{x})\, \partial \bar{C}/\partial t, (14)$$

$$D_\varepsilon = H(\vec{x})D + \big(1 - H(\vec{x})\big)\varepsilon I,$$

where *I* is the identity tensor.

The sorption kinetic equation (6) retains its form in the physical domain:

$$\partial \bar{C}(\vec{x}, t)/\partial t = \beta(C(\vec{x}, t) - \bar{C}(\vec{x}, t)/K_d). (15)$$

In the fictitious domain ($\vec{x} \in \Omega_f$), the following condition is imposed: $\bar{C}(\vec{x}, t) = 0$.

© 2026 by the author(s). Distributed under a Creative Commons CC BY license.

Preprints.org (www.preprints.org) | NOT PEER-REVIEWED | Posted: 27 March 2026 doi:10.20944/preprints202603.2235.v1



Due to the nonlinearity of the governing equations, the system of equations (12), (14), and (15), together with boundary conditions (7)–(9), (13), and initial conditions (10), is solved simultaneously using numerical methods.

The numerical solution procedure in the regular computational domain $R$ at each time step is organized as follows.

1. The pressure field is obtained numerically from Equation (12) with boundary conditions (7)–(9) and (13). The nonlinear elliptic equation for pressure is solved using the **Ritz method** [29].
2. After determining the pressure field, the velocity field is calculated using the relation
$$\phi\vec{v} = -\nabla P/(\alpha_1 + \alpha_2 \mathrm{f}(|\nabla P|)\,.$$
3. The concentration of the mineral in the liquid phase is then determined from the transport equation (14) with boundary and initial conditions (8)–(10). The equation is solved numerically using the **Crank–Nicolson scheme** [22].
4. Finally, the time step is completed by solving the ordinary differential equation describing sorption kinetics (6) with the initial condition (10). Since the concentration of the mineral in the liquid phase $C^{n+1}$ is known at each time step, the kinetic equation of sorption is solved **analytically.**

In this work, a numerical study was carried out to investigate the influence of the presence of a **conical flow distributor** at the inlet of the sorber, its geometrical parameters, and the volumetric flow rate of the solution on the characteristics of the sorption process.

Due to the axial symmetry of the problem with respect to the Oz axis, the calculations were performed in a rectangular computational domain

$$0 < r < R, 0 < z < H$$

using a finite-difference grid of size **150 × 600.**

The influence of the conical distributor geometry and the solution flow rate on the efficiency of the sorption column and the completeness of the ion-exchange process was investigated for the following cases:

1. absence of a conical flow distributor, with volumetric flow rate $Q_0$=0.35 $m^3/h$;
2. a fixed apex position of the conical distributor with opening angles $\alpha$=45$^0$ and 60$^0$, $Q_0$=0.35 $m^3/h$;
3. different flow rates of the solution $Q_0$=0.35 $m^3/h$ and $Q_0$=0.7 $m^3/h$ with the same distributor angle $\alpha$=45$^0$.

The geometric and operating parameters of the sorption column were chosen close to those used in industrial practice: $H$=6 $m$, $R$=$D$/2=1.5 $m$, $d$=0.3 $m$, $\delta$ =0.5 $mm$.

## 3. Results

### *3.1. Flow Structure Without a Conical Distributor*

Figures 4–8 show the calculated spatial distributions of pressure, flow velocity, and mineral concentration in the immobile phase (sorbent) in the absence of the conical distributor at a flow rate $Q_0$=0.35 $m^3/h$.

Figure 4 presents the calculated pressure distribution ($kPa$) and the Reynolds number distribution. The Reynolds number was calculated using the diameter of the inlet pipe $Re = V_0\rho d/\mu$; when calculated based on the diameter of the resin granules, its value is two orders of magnitude smaller. As expected, near the inlet pipe, whose cross-sectional area is ($D$/$d$)$^2$ times smaller than that of the column, both pressure and flow velocity are significantly higher than in the regions farther away from the inlet.

Figure 5 shows the distributions of mineral concentration in the immobile phase after 10 and 40 hours of sorber operation. It can be seen that the main flow containing dissolved uranium species develops in the central part of the column, whereas the near-wall region of the sorbent is involved in the sorption process much more weakly.

© 2026 by the author(s). Distributed under a Creative Commons CC BY license.

Preprints.org (www.preprints.org) | NOT PEER-REVIEWED | Posted: 27 March 2026 doi:10.20944/preprints202603.2235.v1



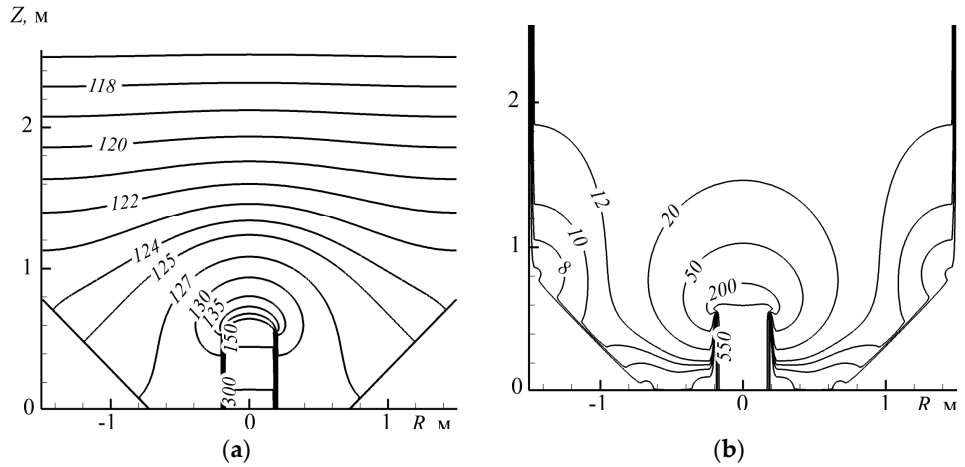


**Figure 4.** (a) Pressure distribution in the liquid (mobile) phase (*kPa*); (b) Reynolds number distribution of the fluid flow in the pores, $Q_0$=0.35 m³/h.

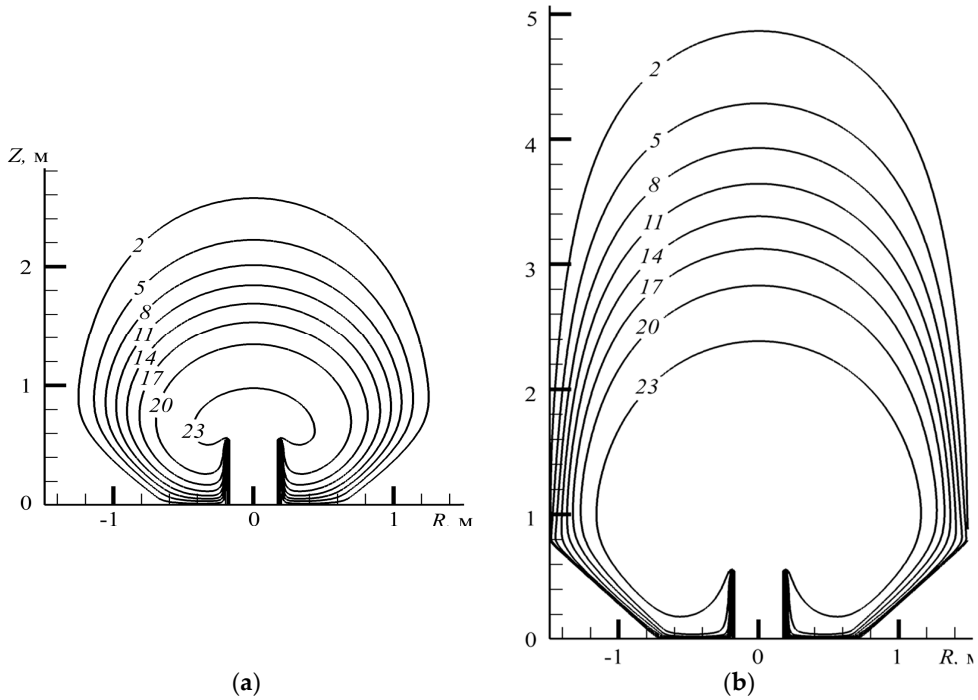


**Figure 5.** Distribution of uranium concentration in the immobile phase (g/l) after (a) 10 *h* and (b) 40 *h* of sorber operation. $Q_0$=0.35 *m³/h*.

This effect is particularly evident in Figure 6, which shows the distribution of mineral concentration in the immobile phase across the column cross-section at the level z=1.5*m* at different times after the beginning of the sorption process. The results indicate that the average mineral concentration across the column cross-section

$$\overline{C}_Z(Z,t) = \int_0^{R(Z)} r\bar{C}(z,r,t)dr/(\pi R^2(Z)).$$

does not exceed 60% of the maximum possible concentration (23 g/l) (see Figures 6 and 7).

© 2026 by the author(s). Distributed under a Creative Commons CC BY license.

Preprints.org (www.preprints.org) | NOT PEER-REVIEWED | Posted: 27 March 2026 doi:10.20944/preprints202603.2235.v1



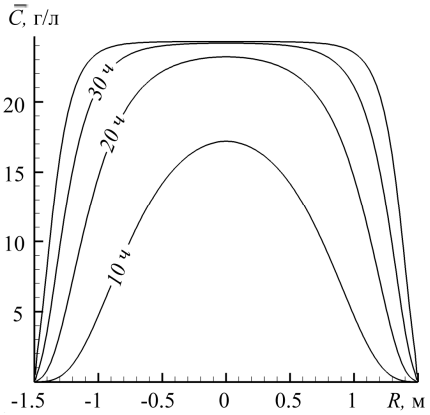


**Figure 6.** Cross-sectional distribution of uranium concentration in the immobile phase at the level $z$=1.5$m$ at different times.

To assess the efficiency of sorbent utilization, the degree of sorbent involvement in the sorption process was analyzed. Particular attention was given to the uniformity of sorption across the column cross-section, which represents a standard criterion used in the operational analysis of industrial sorption columns.

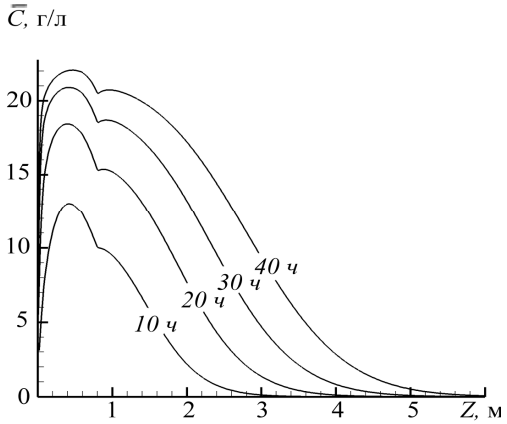


**Figure 7.** Temporal evolution of the cross-sectionally averaged uranium concentration in the immobile phase.

For this purpose, the ratio between the total mass of sorbed mineral in the sorbent layer of height

$$M(z,t) = \int_0^z \int_0^{R(z)} r\bar{C}(z,r,t)\, drdz$$

and the maximum possible mass that can be retained by the sorbent in the same volume

$$M_m(z,t) = \int_0^z \int_0^{R(z)} r\, \bar{C}_{max}(r,z,t) drdz = V_C K_d C_{in}$$

was calculated. Here $V_C$ =$V_C$($z$) denotes the volume of the column segment of height $z$. Figure 8 shows the dependence of the ratio

$$\mu(z,t) = M(z,t)/M_m(z,t)$$

on the height of the column and time.

© 2026 by the author(s). Distributed under a Creative Commons CC BY license.

Preprints.org (www.preprints.org) | NOT PEER-REVIEWED | Posted: 27 March 2026 doi:10.20944/preprints202603.2235.v1



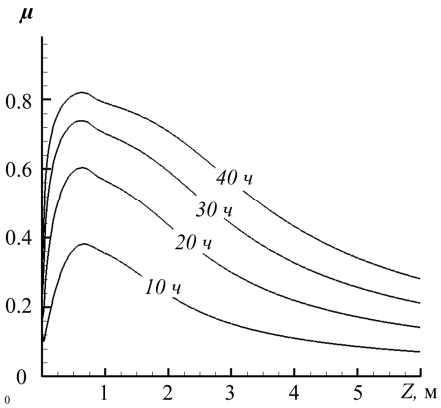


**Figure 8.** Degree of sorbent involvement in the sorption process as a function of column height and time.

Thus, in the absence of a conical distributor, the main flow containing dissolved uranium species is concentrated in the central region of the column, whereas the near-wall sorbent zone participates significantly less in the sorption process. As a result, the average mineral concentration across the column cross-section does not exceed two-thirds of the equilibrium concentration.

The analysis of the sorbent utilization factor also indicates low efficiency of sorbent usage in the column under these conditions.

*3.2. Influence of the Conical Distributor*

Further analysis considered sorber designs with conical distributors having angles $\alpha$=45$^0$ and 60$^0$ at the flow rate $Q_0$=0.35 m$^3$/h.

Figures 9–16 show the calculated distributions of pressure, filtration velocity, and mineral concentration in the solid phase.

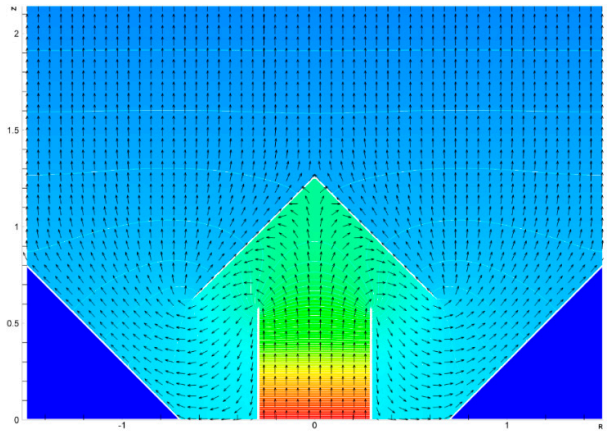

**Figure 9.** Velocity vectors and pressure field in the vicinity of the inlet pipe and the conical flow distributor. Arrows indicate the direction and magnitude of the local velocity; the color scale represents the pressure distribution.

Figure 9 illustrates detailed velocity and pressure fields near the inlet pipe and the conical distributor for the opening angle 2$\alpha$=90$^0$.

Figures 10–11 present the distributions of pressure and the local Reynolds number in the column. The Reynolds number is defined based on the inlet pipe diameter: $Re = Vd\rho/\mu$.

The results show that both pressure and the local Reynolds number decrease rapidly in the vicinity of the conical distributor. For larger opening angles, the pressure drop near the cone is

© 2026 by the author(s). Distributed under a Creative Commons CC BY license.

Preprints.org (www.preprints.org) | NOT PEER-REVIEWED | Posted: 27 March 2026 doi:10.20944/preprints202603.2235.v1



slightly greater; however, farther downstream the pressure fields in both cases become nearly identical.

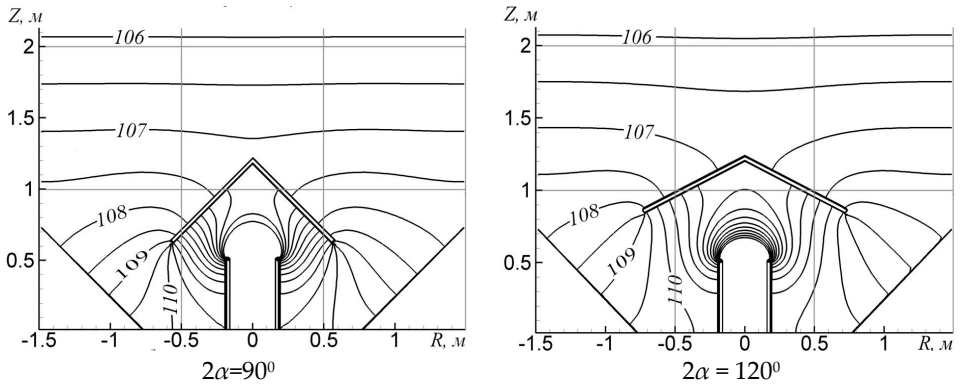


**Figure 10.** Pressure isolines in the liquid phase inside the sorption column for distributor opening angles $2\alpha$ = $90^0$ and $2\alpha$ =$120^0$, $Q_0$=0.35 m³/h.

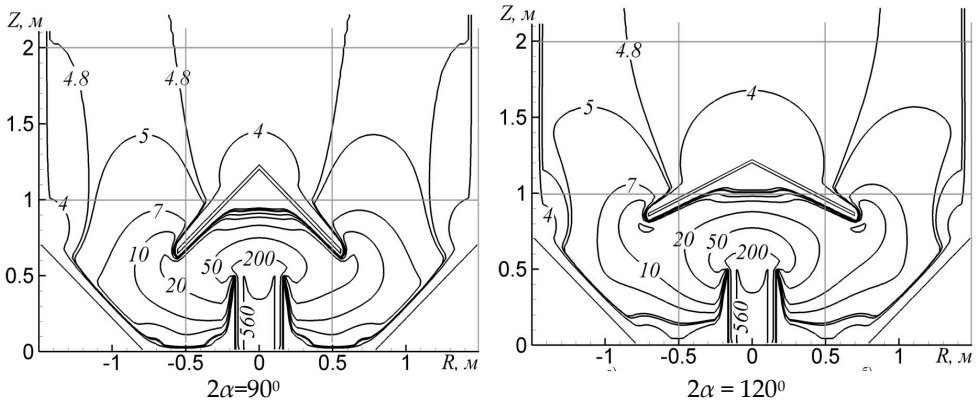


**Figure 11.** Isolines of the local Reynolds number of the fluid flow in the pores for distributor opening angles $2\alpha$ = $90^0$ and $2\alpha$ =$120^0$, $Q_0$=0.35 m³/h.

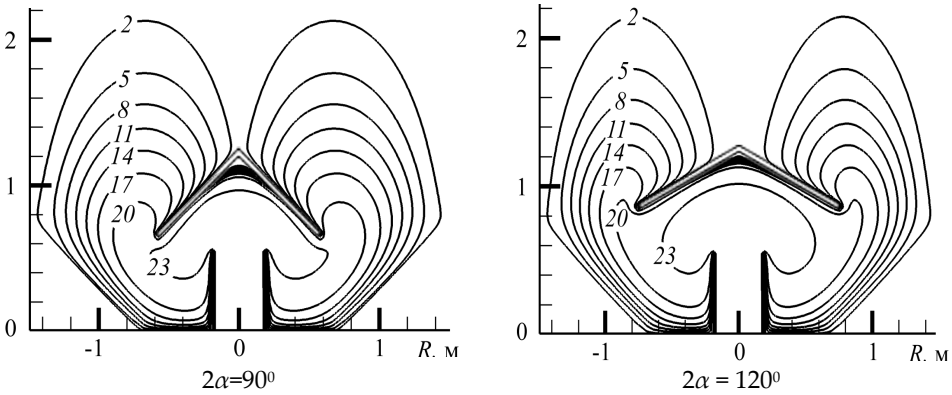


**Figure 12.** Distribution of uranium concentration in the solid phase after 10 *h* of column operation for distributor opening angles $2\alpha$ = $90^0$ and $2\alpha$ = $120^0$, $Q_0$ =0.35 м³/ч. Numbers on the isolines correspond to the mass concentration (g/l).

Figures 12 and 13 show the distributions of mineral concentration in the solid phase after 10 and 40 hours of column operation. The results indicate that for larger distributor opening angles the saturation zone extends farther along the column. At the same time, the region directly behind the distributor that is not involved in sorption becomes wider compared to the case of smaller angles.

© 2026 by the author(s). Distributed under a Creative Commons CC BY license.

Preprints.org (www.preprints.org) | NOT PEER-REVIEWED | Posted: 27 March 2026 doi:10.20944/preprints202603.2235.v1



The mineral concentration in each cross-section of the column gradually increases with time until reaching the equilibrium concentration, which follows directly from the sorption kinetics equation (6).

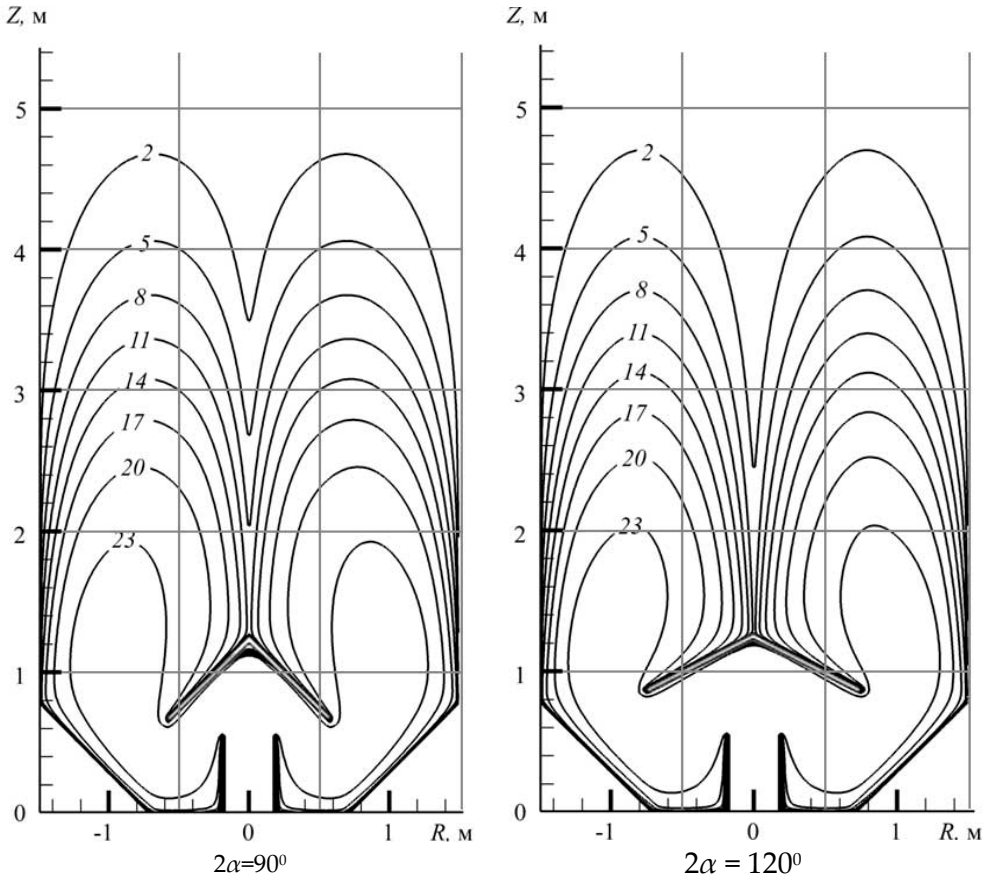


**Figure 13.** Distribution of uranium concentration in the solid phase after 40 h of column operation for distributor opening angles $2\alpha = 90^0$ и $2\alpha = 120^0$. Numbers on the isolines correspond to the mass concentration (g/l).

Analysis of the concentration profiles shows that the distribution of mineral concentration in the solid phase forms a sorption saturation wave propagating along the column in the direction of the flow. The front of this wave gradually broadens due to longitudinal hydrodynamic dispersion in the porous sorbent bed.

Figure 14 shows the cross-sectional distribution of uranium concentration in the solid phase at the level $z$=1.5 m from the inlet of the sorption column at different times and for different opening angles of the distributor. It can be seen that for the angle $2\alpha=120^0$ the saturation wave propagates farther along the column than in the case of $2\alpha=90^0$.

The distribution of the cross-sectionally averaged concentration of uranium adsorbed by the sorbent along the column height is determined by

$$\overline{C}_z(z,t) = \frac{1}{\pi R^2(z)} \int_0^{R(z)} r\bar{C}(z,r,t)dr.$$

Figure 15 shows the distribution of the averaged concentration $\overline{C}_z$ at different times for different opening angles of the distributor. The influence of the distributor opening angle on the overall character of the concentration distribution is relatively small and becomes noticeable mainly at the initial stage of the process. In the case of a narrower distributor ($2\alpha=90^0$), a more intensive adsorption of uranium is observed. This effect is associated with the higher filtration velocity of the solution in the corresponding region of the sorption column (see Figure 11).

© 2026 by the author(s). Distributed under a Creative Commons CC BY license.

Preprints.org (www.preprints.org) | NOT PEER-REVIEWED | Posted: 27 March 2026 doi:10.20944/preprints202603.2235.v1



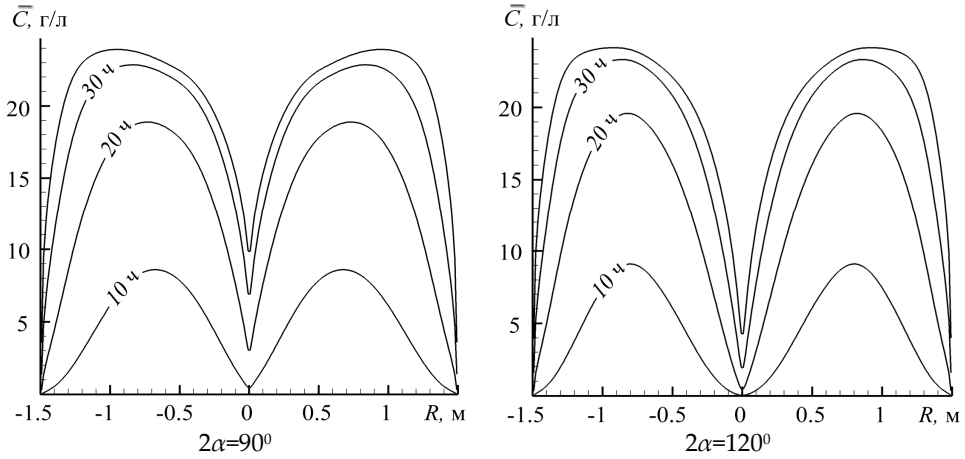


**Figure 14.** Cross-sectional distribution of uranium concentration in the solid phase at the level $z$ =1.5 m for different distributor opening angles.

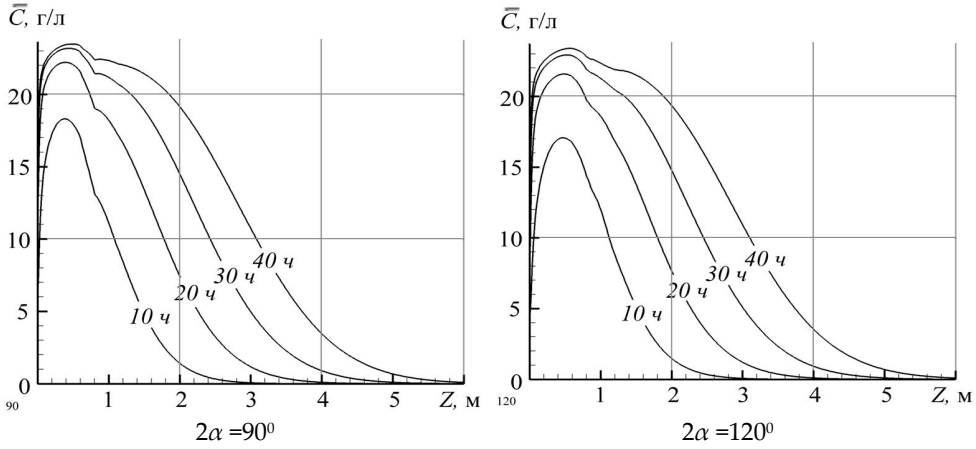


**Figure 15.** Distribution of the cross-sectionally averaged uranium concentration in the solid phase along the column height at different times for distributor opening angles $2\alpha = 90^0$ и $2\alpha = 120^0$, $Q_0$=0.35 м³/ч.

This feature is also clearly illustrated in Figure 16, which shows the distribution of the degree of sorbent involvement in the sorption process along the column height for different opening angles of the conical distributor.

Based on the performed analysis, it can be concluded that the **non-uniform distribution of dissolved uranium species across the column cross-section** indicates incomplete sorption and therefore insufficient efficiency of the column operation. In particular,

1. the main volume of uranium in both the mobile and immobile phases forms a **ring-shaped cylindrical region** whose thickness is approximately two times smaller than the column radius;
2. the mass concentration of uranium in the central part of the column in both phases is significantly lower than the equilibrium saturation concentration of the sorbent;
3. the conical flow distributor installed at the inlet of the column does not ensure a sufficiently uniform distribution of the solution across the column cross-section.

These results indicate that the efficiency of sorbent utilization in the column is largely controlled by the **hydrodynamic structure of the flow**, which determines the spatial distribution of mass transfer in the porous sorbent bed.

© 2026 by the author(s). Distributed under a Creative Commons CC BY license.

Preprints.org (www.preprints.org) | NOT PEER-REVIEWED | Posted: 27 March 2026 doi:10.20944/preprints202603.2235.v1



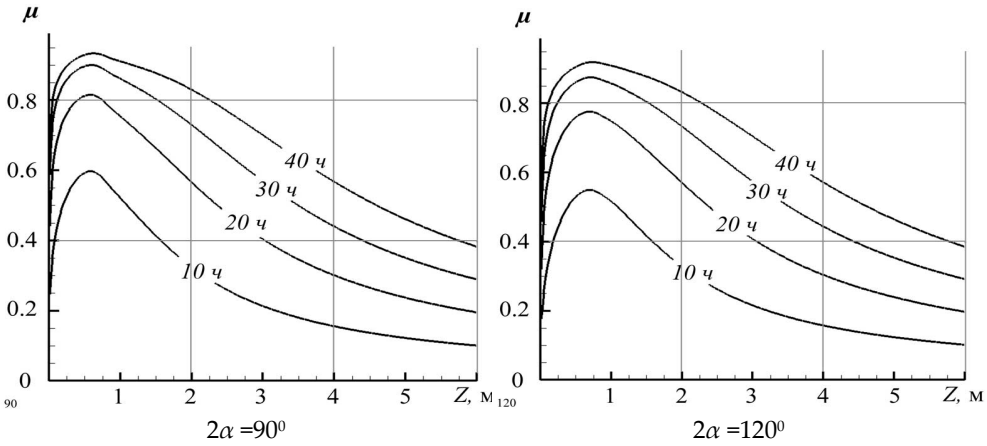


**Figure 16.** Distribution of the degree of sorbent involvement in the sorption process along the column height for different distributor opening angles: $2\alpha = 90^0$ и $2\alpha = 120^0$, $Q_0$=0.35 м³/ч.

*3.3. Influence of Flow Rate*

Figures 17–21 present the results of a comparative analysis of the sorption column operation at two solution flow rates: $Q_0$=0.35 m³/h и $Q_0$=0.7 m³/h. In all cases, the opening angle of the conical distributor is $2\alpha$=90⁰.

With increasing solution flow rate, the pressure gradient and therefore the hydraulic resistance of the resin bed increase significantly. A considerable part of the pressure drop occurs in the region between the inlet pipe and the flow distributor, where the liquid velocity is the highest (Figure 17). The local Reynolds number decreases sharply behind the conical distributor in both columns (Figures 17–18).

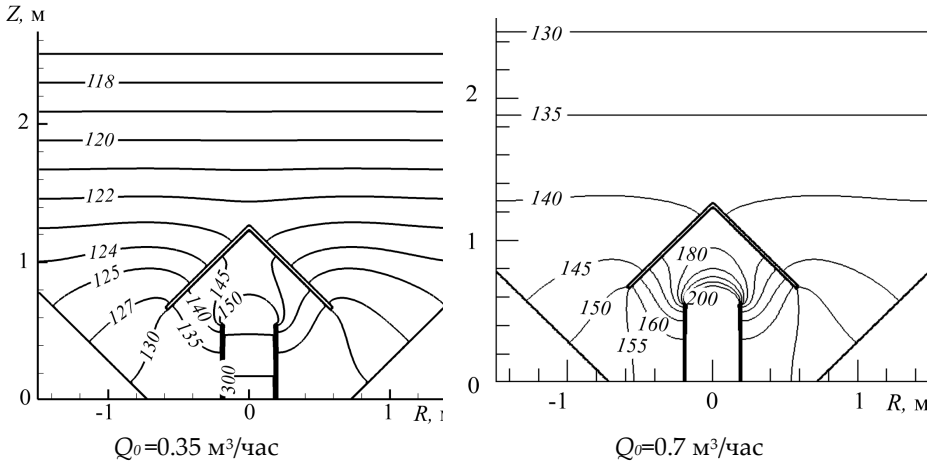


**Figure 17.** Pressure isolines in the liquid phase inside the column for different solution flow rates *(kPa)*.

For efficient operation of the sorption column, the Damköhler number $Da = \beta H/V$ must satisfy the condition $Da \geq 1$ which ensures the formation of a narrow mass-transfer zone and efficient column operation (Bird et al.).

For practical values of the system parameters

$$\beta = 120\ h^{-1},\ \varphi = 0.35,\ H=6m,\ R=1.5m,\ S=\pi R^2,\ Q>0.35\ m^3/h,\ V=Q/(\varphi S),$$

the hydrodynamic residence time of the solution in the column is much larger than the characteristic sorption time, therefore, $Da \gg 1$. This means that sorption occurs much faster than convective transport. Consequently, the structure of the mass-transfer zone is mainly determined by flow hydrodynamics and longitudinal dispersion.

© 2026 by the author(s). Distributed under a Creative Commons CC BY license.

Preprints.org (www.preprints.org) | NOT PEER-REVIEWED | Posted: 27 March 2026 doi:10.20944/preprints202603.2235.v1



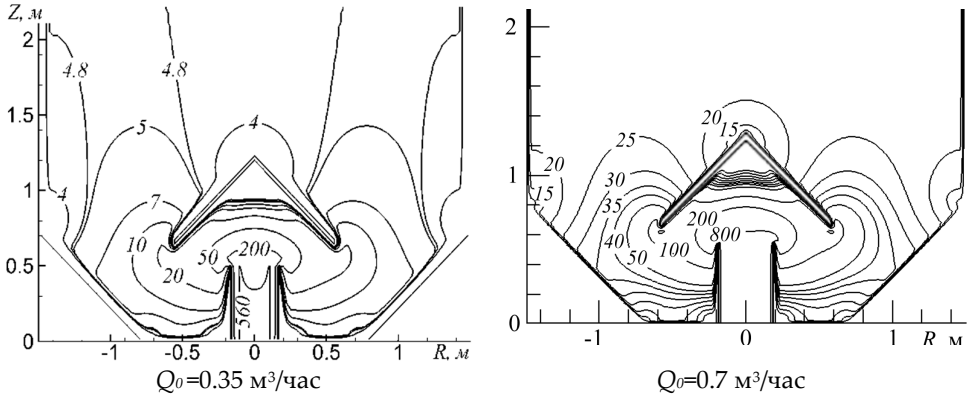


**Figure 18.** Isolines of the local Reynolds number of fluid flow in the pores for different solution flow rates.

Figures 19 and 20 illustrate the distributions of mineral concentration in the mobile (liquid) and immobile (adsorbed) phases at two different times. For the considered parameters of the sorption column, the ion-exchange sorption of dissolved uranium species occurs almost instantaneously compared with convective transport. Therefore, the ion-exchange process is primarily hydrodynamically controlled.

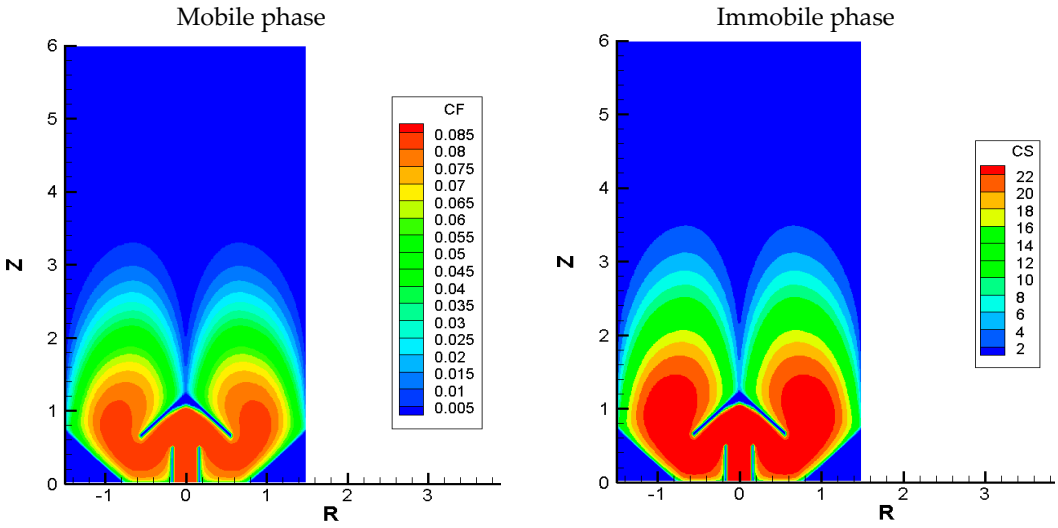


**Figure 19.** Spatial distributions of uranium concentration in the mobile (liquid) and immobile (adsorbed) phases at the time $t = t_1$.

© 2026 by the author(s). Distributed under a Creative Commons CC BY license.

Preprints.org (www.preprints.org) | NOT PEER-REVIEWED | Posted: 27 March 2026 doi:10.20944/preprints202603.2235.v1



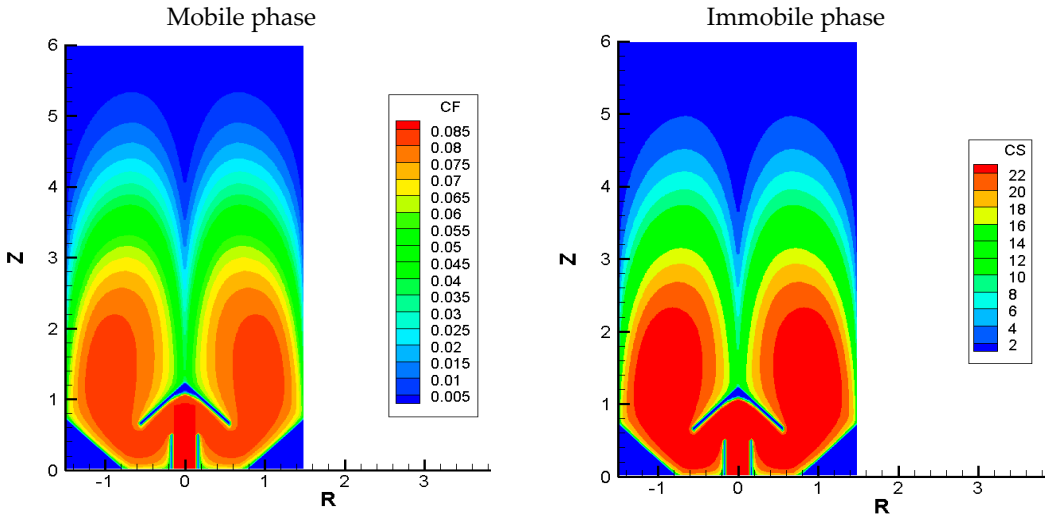


**Figure 20.** Spatial distributions of uranium concentration in the mobile (liquid) and immobile (adsorbed) phases at the time $t=t_2$.

The calculations also show that doubling the solution flow rate (i.e., the average linear velocity) leads to an increase in the width of the sorption front (the mass-transfer zone) by approximately 1.5 times (Figure 20). This effect is caused by the increase in the longitudinal dispersion coefficient, which is proportional to the flow velocity.

At the same time, excessive increase in the solution flow rate results in a substantial rise in the hydraulic resistance of the resin bed and consequently increases energy consumption.

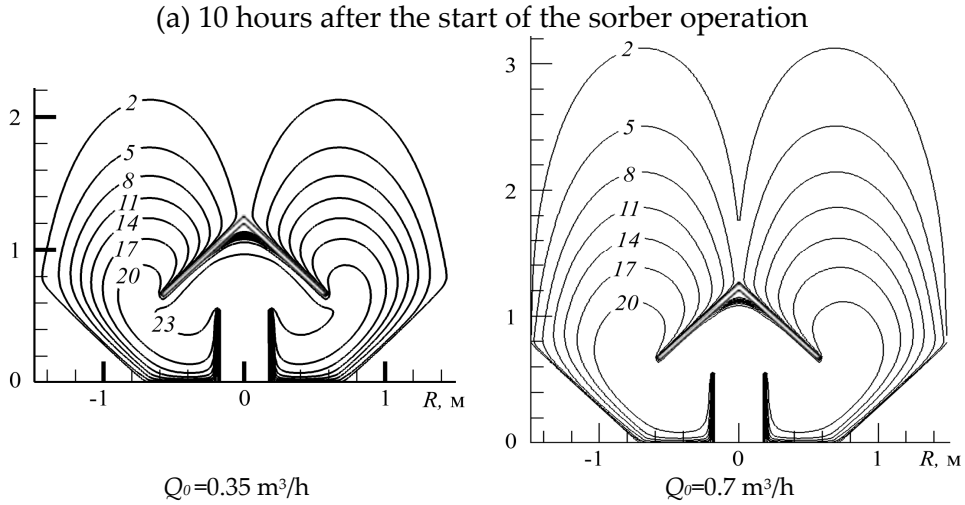


© 2026 by the author(s). Distributed under a Creative Commons CC BY license.

Preprints.org (www.preprints.org) | NOT PEER-REVIEWED | Posted: 27 March 2026 doi:10.20944/preprints202603.2235.v1



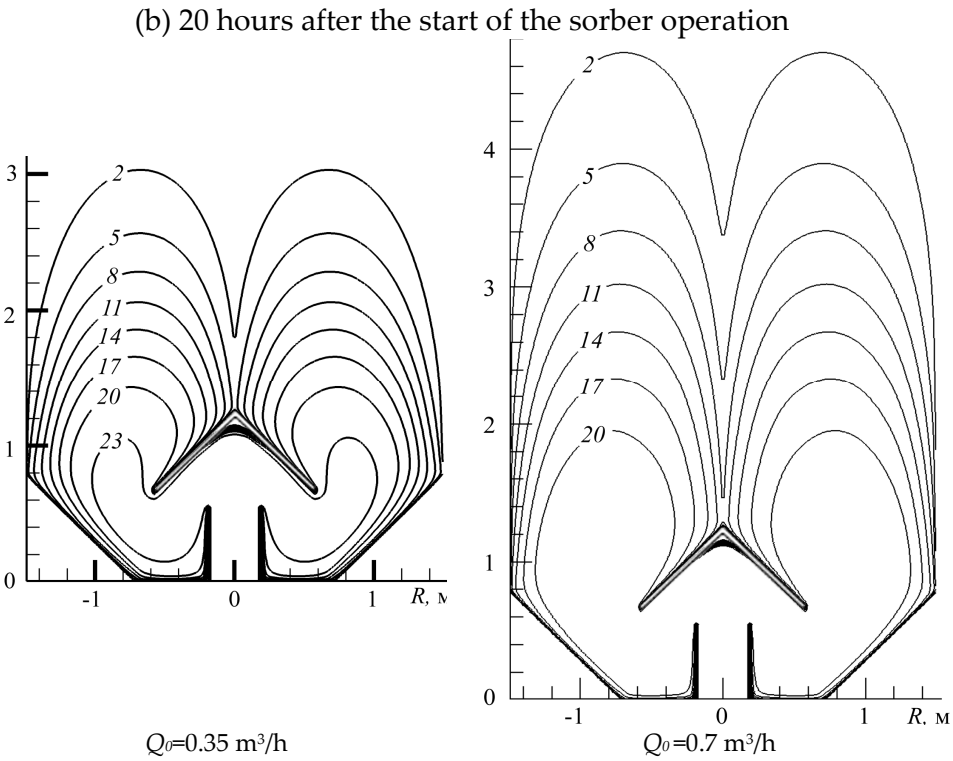


**Figure 20.** Distribution of uranium concentration in the immobile phase for different solution flow rates after (a) 10 *h* and (b) 20 *h* of column operation. Numbers on the isolines correspond to the mass concentration (*g*/*l*).

## 4. Discussion

The present study develops a coupled physical, mathematical, and numerical model describing uranium oxide sorption from productive solutions in a packed ion-exchange column equipped with a conical flow distributor. The hydrodynamic behavior of the liquid phase in the porous sorbent bed was described using the Forchheimer filtration law combined with the mass conservation equation, while mass transfer between the solution and the ion-exchange resin was modeled using a convective–dispersion transport equation coupled with a sorption kinetics equation. Numerical simulations were carried out using the fictitious domain method, which allows efficient modeling of transport processes in geometrically complex domains.

The obtained results confirm that the hydrodynamic structure of the flow plays a key role in determining the efficiency of ion-exchange sorption processes in packed columns. In particular, the calculations demonstrate that the absence of a flow distributor leads to strong non-uniformity of the velocity field and, consequently, to uneven utilization of the sorbent bed. The main solution stream tends to concentrate in the central part of the column, whereas the near-wall region remains weakly involved in the sorption process. As a result, the average sorbent loading does not exceed approximately 60% of the equilibrium capacity, indicating incomplete utilization of the sorbent layer.

Such behavior is consistent with the general understanding of hydrodynamic heterogeneity in packed columns reported in previous studies of reactive transport and sorption processes in porous media. In many industrial sorption systems, non-uniform flow distribution leads to channeling and preferential flow paths, which significantly reduce mass-transfer efficiency and increase operational costs. The present modeling results confirm that similar effects may occur in uranium recovery columns when the inlet flow is not properly distributed.

The introduction of a conical flow distributor substantially modifies the hydrodynamic structure of the flow. Numerical simulations show that the pressure and the local Reynolds number decrease sharply in the region of the distributor and then rapidly become more uniform along the column height. The geometry of the distributor significantly affects the spatial development of the sorption

© 2026 by the author(s). Distributed under a Creative Commons CC BY license.

Preprints.org (www.preprints.org) | NOT PEER-REVIEWED | Posted: 27 March 2026 doi:10.20944/preprints202603.2235.v1



zone. In particular, larger opening angles of the distributor lead to a wider spatial distribution of the sorption zone along the column, although at the initial stage of operation the degree of sorbent involvement may be slightly lower due to higher filtration velocities near the distributor.

The results also demonstrate that the spatial distribution of uranium concentration within the column forms a ring-shaped region of active sorption between the central and near-wall zones. This feature reflects the combined influence of radial velocity gradients and longitudinal dispersion. Such non-uniform patterns indicate that hydrodynamic factors strongly influence the structure of the mass-transfer zone even when sorption kinetics are relatively fast.

An important finding of the study is that the Damköhler number for the considered operating conditions significantly exceeds unity. This implies that the ion-exchange reaction proceeds much faster than convective transport. Consequently, the formation and propagation of the mass-transfer zone are mainly governed by hydrodynamic dispersion and flow structure rather than by intrinsic reaction kinetics. This conclusion is consistent with theoretical analyses of reactive transport in porous media, where transport-controlled regimes dominate when reaction rates are sufficiently high.

The influence of the solution flow rate was also analyzed. The simulations indicate that doubling the flow rate results in an approximately 1.5-fold increase in the width of the sorption front. This behavior is associated with an increase in longitudinal dispersion and enhanced mixing within the porous medium. However, increasing the flow rate also leads to a higher pressure gradient and greater hydraulic resistance of the resin bed, which in turn increases energy consumption for pumping the solution. Therefore, optimization of operating conditions requires balancing improved mass transfer against increased energy costs.

Another important practical outcome of the developed model is the possibility of estimating the height of the saturated sorbent layer at the moment when the uranium concentration in the outlet solution reaches its allowable limit. This provides a useful tool for determining optimal operational cycles and for planning the unloading of saturated sorbent in industrial sorption systems.

The developed modeling framework can therefore be applied to analyze the performance of industrial sorption columns used in uranium recovery operations. In particular, it can assist in optimizing the design of inlet distributors, improving the uniformity of flow distribution, and enhancing the overall utilization efficiency of ion-exchange resins.

Future research should focus on several directions. First, further investigation of alternative distributor geometries and multi-stage flow distribution systems could help achieve more uniform radial flow profiles. Second, coupling the present model with detailed pore-scale transport models may improve the description of dispersion and sorption kinetics in heterogeneous resin beds. Finally, integration of the model with real industrial operating data would enable more accurate calibration of model parameters and facilitate predictive simulations for large-scale sorption systems.

## 5. Conclusions

A coupled hydrodynamic and mass-transfer model describing uranium sorption in a packed ion-exchange column equipped with a conical flow distributor has been developed. The model combines the Forchheimer filtration law with a convective–dispersion transport equation and a sorption kinetics model, allowing detailed analysis of hydrodynamic and mass-transfer processes in columns of complex geometry.

The main conclusions of the study are as follows:

1. The hydrodynamic structure of the flow in the sorption column strongly depends on the presence and geometry of the inlet flow distributor. In the absence of a distributor, the main flow develops in the central part of the column, while the near-wall region of the sorbent bed participates in the sorption process much more weakly.
2. The spatial distribution of uranium concentration within the column forms a ring-shaped zone of active sorption, indicating non-uniform utilization of the sorbent bed.

© 2026 by the author(s). Distributed under a Creative Commons CC BY license.

Preprints.org (www.preprints.org) | NOT PEER-REVIEWED | Posted: 27 March 2026 doi:10.20944/preprints202603.2235.v1



3. For the considered operating conditions, the Damköhler number is significantly greater than unity, which indicates that the ion-exchange reaction proceeds much faster than convective transport. Under these conditions, the structure of the mass-transfer zone is mainly governed by hydrodynamic dispersion.
4. Increasing the solution flow rate by a factor of two leads to an approximately 1.5-fold increase in the width of the mass-transfer zone due to enhanced longitudinal dispersion, while simultaneously increasing hydraulic resistance and energy consumption.
5. The developed numerical approach can be used for analyzing the performance of industrial sorption columns and for optimizing their design and operating conditions in uranium recovery processes.

**Author Contributions:** Conceptualization, A.K.; methodology, A.K. and Z.U.; software, Z.U. and A.B.; validation, A.K., Z.U. and A.B.; formal analysis, A.K. and Z.U.; investigation, Z.U. and A.B.; resources, A.K.; data curation, Z.U.; writing—original draft preparation, A.K.; writing—review and editing, A.K.; visualization, Z.U. and A.B.; supervision, A.K.; project administration, A.K.; funding acquisition, A.K. All authors have read and agreed to the published version of the manuscript.

**Funding: This work was supported by the** Ministry of Science and Higher Education of the Republic of Kazakhstan [grant No. **BR31715767 and BR28713691**].

**Data Availability Statement:** The funding agency has limited access to the numerical results of this study to protect confidential information.

**Conflicts of Interest:** The authors declare no conflicts of interest. The funders had no role in the design of the study; in the collection, analyses, or interpretation of data; in the writing of the manuscript; or in the decision to publish the results.

## Abbreviations

The following abbreviations are used in this manuscript:

| | |
|---|---|
| SK | Sorption column |
| ISL | In-situ leaching |
| **FDM** | **Fictitious domain method** |

## References

1. Mamilov, M.A. (Ed.). Dobycha urana metodom podzemnogo vyshchelachivaniya [Uranium mining by in-situ leaching]. Moscow: Atomizdat, 1980. (in Russian).
2. Wang, B.; Li, X.; Zhang, Y.; et al. Ion migration in in-situ leaching (ISL) of uranium: Field trial and reactive transport modelling. ***J. Hydrol***. **2022**, ***615***, 128634.
3. Collet, A.; Regnault, O.; Ozhogin, A.; Imantayeva, A.; Garnier, L. Three-dimensional reactive transport simulation of uranium in situ recovery: Large-scale well field applications in Shu Saryssu Basin, Tortkuduk deposit (Kazakhstan). **Hydrometallurgy** 2022, 211, 105873. https://doi.org/10.1016/j.hydromet.2022.105873.
4. Kurmanseiit, M.B.; Tungatarova, M.S.; Kaltayev, A.; Royer, J.-J. Reactive transport modeling during uranium in situ leaching (ISL): The effects of ore composition on mining recovery. ***Minerals*** **2022**, ***12,*** *1340*. https://doi.org/10.3390/min12111340.
5. Kurmanseiit, M.B.; Tungatarova, M.S.; Royer, J.-J.; Aizhulov, D.Y.; Shayakhmetov, N.M.; Kaltayev, A. Streamline-based reactive transport modeling of uranium mining during in-situ leaching: Advantages and drawbacks. ***Hydrometallurgy*** **2023**, **220**, *106107*. https://doi.org/10.1016/j.hydromet.2023.106107.
6. Li, Y.; Zhang, C.; Tang, Z.; Li, C.; Liu, Z.; Tan, K.; Liu, L. Hydrodynamics control for the well field of in-situ leaching of uranium. ***Nucl. Eng. Technol.*** **2024**. https://doi.org/10.1016/j.net.2024.05.021.
7. Couper, J.R.; Penney, W.R.; Fair, J.R.; Walas, S.M. *Chemical Process Equipment: Selection and Design*; Elsevier: Amsterdam, The Netherlands, 2012.

© 2026 by the author(s). Distributed under a Creative Commons CC BY license.

Preprints.org (www.preprints.org) | NOT PEER-REVIEWED | Posted: 27 March 2026 doi:10.20944/preprints202603.2235.v1




8. Orrego, P.; Hernández, J.; Reyes, A. Uranium and molybdenum recovery from copper leaching solutions using ion exchange. ***Hydrometallurgy*** **2019**, ***184,*** 116–122. https://doi.org/10.1016/j.hydromet.2018.12.021.
9. Quinn, J.E.; Sedger, D.S.; Brennan, A.T.; Ring, R.; Soldenhoff, K. Recovery of uranium from carbonate solutions using Lewatit TP 107 resin. **Hydrometallurgy 2020**, ***194***, 105360. https://doi.org/10.1016/j.hydromet.2020.105360.
10. Zhang, F.; Luo, W.; Parker, J.; Brooks, S.; Watson, D.; Jardine, P.; Gu, B. Modeling uranium transport in acidic contaminated groundwater with base addition. ***J. Hazard. Mater.*** **2011**, ***190,*** 863–868. https://doi.org/10.1016/j.jhazmat.2011.04.022.
11. Mahmoud, M. Kinetics studies of uranium sorption by powdered corn cob in batch and fixed bed systems. J. ***Adv. Res.*** **2015**, ***6***, 487–495. https://doi.org/10.1016/j.jare.2015.02.004.
12. Patel, H. Fixed-bed column adsorption study: A comprehensive review. ***Appl. Water Sci.*** **2019**, ***9***, 45. https://doi.org/10.1007/s13201-019-0927-7.
13. Baqer, Y.; Thornton, S.; Stewart, D.; Norris, S.; Chen, X. Analysis of uranium sorption in a laboratory column experiment using a reactive transport and surface complexation model. ***Transp. Porous Media*** **2023**, ***149***, 423–452. https://doi.org/10.1007/s11242-023-01956-y.
14. Bear, J.; Zaslavsky, D.; Irmay, S. *Physical Principles of Water Percolation and Seepage*; Elsevier: New York, NY, USA, 1972.
15. Collins, R.E. *Flow of Fluids through Porous Materials*; Reinhold: New York, NY, USA, 1961.
16. Goldshtik, M.A. *Transport Processes in Granular Media*; Institute of Thermophysics SB RAS: Novosibirsk, Russia, 1984.
17. Shestakov, V.M. *Hydrogeodynamics*; Moscow State University Press: Moscow, Russia, 1995.
18. Ruthven, D.M. Principles of Adsorption and Adsorption Processes; Wiley: New York, NY, USA, 1984.
19. Bird, R.B.; Stewart, W.E.; Lightfoot, E.N. *Transport Phenomena*, 2nd ed.; Wiley: New York, NY, USA, 2002.
20. Helfferich, F. *Ion Exchange*; Dover Publications: New York, NY, USA, 1995.
21. Simonin, J.-P. On the comparison of pseudo-first-order and pseudo-second-order rate laws in the modeling of adsorption kinetics. ***Chem. Eng. J.*** **2016**, ***300,*** 254–263. https://doi.org/10.1016/j.cej.2016.04.079.
22. Fletcher, C.A.J. *Computational Techniques for Fluid Dynamics*, Vol. 2; Springer: Berlin, Germany, 1991.
23. Morianou, G.; Kourgialas, N.N.; Karatzas, G.P. A review of HYDRUS-2D/3D applications for simulations of water dynamics, root uptake and solute transport. ***Water*** **2023**, ***15***, *741*. https://doi.org/10.3390/w15040741.
24. Šimůnek, J.; Brunetti, G.; Jacques, D.; van Genuchten, M.T.; Šejna, M. Development and applications of the HYDRUS software packages since 2016. ***Vadose Zone J***. **2024**, ***23***. https://doi.org/10.1002/vzj2.20310.
25. Vabishchevich, P.N. The Fictitious Domain Method in Problems of Mathematical Physics, 2nd ed.; Fizmatlit: Moscow, Russia, 2017.
26. Thirumalaisamy, R.; Patankar, N.A.; Bhalla, A.P. Treatment of Neumann and Robin boundary conditions in fictitious domain methods. ***J. Comput. Phys.*** **2022**, ***448***, 110726.
27. Corti, D.C.; Delay, G.; Fernández, M.A.; Vergnet, F.; Vidrascu, M. A low-order fictitious domain method with enhanced mass conservation for the Stokes interface problem. ***ESAIM Math. Model. Numer. Anal.*** **2024**, ***58***, 303–333. https://doi.org/10.1051/m2an/2023103.
28. Kale, S.; Pradhan, D.; Kumar, S. Analysis of $H^1$-penalized fictitious domain method for parabolic problems. ***Comput. Math. Appl.*** **2025**, ***196***, 183–200. https://doi.org/10.1016/j.camwa.2025.07.009.
29. Zhivotenko, N. Ritz method. 2021. Available online: https://doi.org/10.13140/RG.2.2.30683.44323.


**Disclaimer/Publisher's Note:** The statements, opinions and data contained in all publications are solely those of the individual author(s) and contributor(s) and not of MDPI and/or the editor(s). MDPI and/or the editor(s) disclaim responsibility for any injury to people or property resulting from any ideas, methods, instructions or products referred to in the content.

© 2026 by the author(s). Distributed under a Creative Commons CC BY license.